Available online at www.sciencedirect.com
ScienceDirect
International Journal of Heat and Mass Transfer 50 (2007) 2406–2413
International Journal of HEAT and MASS TRANSFER
www.elsevier.com/locate/ijhmt

Analysis of laminar dissipative flow and heat transfer in a porous saturated circular tube with constant wall heat flux

Shigeru Tada [a,*], Koichi Ichimiya [b]

[a] Department of Mechanical Engineering and Science, Tokyo Institute of Technology, 2-12-1 Ookayama, Meguro-ku, Tokyo 152-3116, Japan
[b] Interdisciplinary Graduate School of Medicine and Engineering, Mechanical Systems Engineering, University of Yamanashi, 4-3-11 Takeda, Kofu, Yamanashi 400-8511, Japan

Received 15 May 2006; received in revised form 2 October 2006
Available online 20 February 2007

Abstract

A theoretical study of the thermal development of forced convection was performed using a circular tube filled with a saturated porous medium, with constant wall heat flux, and with the effect of viscous dissipation. The solution was obtained using the method of separation of variables. The Sturm–Liouville system was solved for the eigenvalues. Ordinary differential equations for the eigenfunctions were solved numerically by the fourth-order Runge–Kutta method. Results show that, in the presence of the viscous dissipation, both the level and distribution of temperature are altered remarkably, even for small values of the Brinkman number, *Br*, which is the ratio of heat generation caused by viscous dissipation to the value of heat flux at the wall. The value of the local Nusselt number, *Nu*, is demonstrably independent of *Br*, unlike the situation in which the wall temperature remains constant.

Keywords: Porous medium; Forced convection; Thermal development; Brinkman model; Viscous dissipation; Channel

1. Introduction

In recent years, increasing attention has been devoted to problems of forced convection in a porous medium tube because of the increasing practical use of porous media, e.g., hyperporous media used in the cooling of electric equipment [1]. Despite numerous precedent studies of heat transfer in porous media in the past, analytical solutions of the various problems of the thermally developing flow in a pipe with a saturated porous medium were obtained only recently by Haji-Sheikh and Vafai [2] and Nield et al. [3]. In their studies, solutions were obtained using the method of separation of variables. The Sturm–Liouville system was solved for the eigenvalues, and the ordinary differential equations for the eigenfunctions were calculated numerically.

From a practical point of view, the heat generation caused by the viscous dissipation plays a role in the development of the temperature field in the porous medium pipe when the value of the permeability of the porous medium (or Darcy Number, *Da*) takes a considerably small value because the drag force is not negligible in this situation, different from the plain Poiseuille flow. Problems of the transport of heavy oil with a very high Prandtl number, *Pr*, and the context of particle bed nuclear reactors are also relevant cases. However, among the numerous investigations of forced convection in porous media, those that have addressed thermal development associated with viscous dissipation are quite few [4–8]. Nield and coworkers analytically investigated forced convection in a circular tube [4] and a channel bounded by two parallel plates [5,6] that were maintained at constant temperatures. Hooman and Ranjbar-Kani [7] theoretically investigated a similar problem. They solved the problem numerically using an asymptotic solution of the fully developed velocity distribution and found that the fully developed Nusselt number, *Nu*,

* Corresponding author. Tel.: +81 3 5734 2179; fax: +81 3 5734 2893.
E-mail address: stada@mech.titech.ac.jp (S. Tada).

0017-9310/$ - see front matter © 2007 Elsevier Ltd. All rights reserved.
doi:10.1016/j.ijheatmasstransfer.2006.10.049

Nomenclature

Br	Brinkman number $(=\mu w_{\mathrm{m}}^{*2}/q_{\mathrm{w}}R)$
C_p	specific heat [J/kg K]
c_n	coefficients
Da	Darcy number $(=K_p/R^2)$
K_p	permeability [m^2]
M	$=\mu_{\mathrm{e}}/\mu$
Nu	Nusselt number
p	nondimensional pressure
Pe	Peclet number $(=Re\,Pr)$
Pr	Prandtl number
q_{w}	wall heat flux [W/m^2]
R	tube radius [m]
r	nondimensional radial coordinate
Re	Reynolds number $(=\rho R w_{\mathrm{m}}^*/\mu)$
R_n	eigenfunctions
T	temperature [K]
u	nondimensional radial velocity
w	nondimensional axial velocity
w_{m}	nondimensional mean axial velocity
z	nondimensional axial coordinate

Greek symbols

α	$=(M\,Da)^{-\frac{1}{2}}$
κ_{e}	effective thermal conductivity [W/m K]
λ_n	eigenvalues
μ	fluid viscosity [N s/m^2]
μ_{e}	effective viscosity [N s/m^2]
Θ	nondimensional temperature $(=\kappa_{\mathrm{e}}(T-T_0)/q_{\mathrm{w}}R)$
θ	nondimensional temperature
θ_{g}	nondimensional temperature
ρ	density $[\kappa\gamma/\mu^3]$

Subscripts and superscripts

0	flow entrance
m	bulk mean value
w	wall
$*$	dimensional quantities

is independent of the Brinkman number, Br, although the developing Nu depends strongly on the Br. Hooman and coworker [8] also investigated the viscous dissipation effect on forced convection in a porous saturated circular tube with an isoflux wall using perturbation analysis.

In the present study, in a manner similar to that of Nield et al., we solved the problem of thermal development of forced convection in a circular tube filled with a saturated porous medium, with constant wall heat flux, and with the effect of viscous dissipation [3]. In modeling the flow field in a porous medium, the Brinkman flow model [9] was incorporated into momentum equations. The analysis engenders expressions for the local Nu as a function of the nondimensional longitudinal coordinate along the circular tube.

2. Mathematical model development

In the present study, heat and fluid flow in a circular tube filled with a saturated homogeneous porous medium were investigated analytically and numerically. The tube with radius R was aligned with the z-axis whose origin $(z=0)$ corresponds to the entrance of the flow where the velocity and thermal boundary condition were applied (Fig. 1). We assumed that flow was steady and axisymmetric about the center axis of the tube. The uniform heat flux q_{w} was applied over the wall. The direction of the heat flux toward the tube internal area was taken as positive.

The Brinkman momentum equation of the steady state flow in the porous medium of permeability K_p is given as

$$0 = -\frac{\partial p^*}{\partial z^*} + \mu_{\mathrm{e}}\Delta w^* - \frac{\mu}{K_p}w^*, \tag{1}$$

where w^*, p, μ_{e}, μ, and Δ respectively represent the axial flow velocity, the hydraulic pressure, effective viscosity, fluid viscosity, and the Laplace operator. Note that dependent variables with superscript, $(\,)^*$, are dimensional values. The boundary conditions are

$$\left.\begin{aligned} w^*|_{r^*=R} &= 0 \\ \left.\frac{\partial w^*}{\partial r^*}\right|_{r^*=0} &= 0 \end{aligned}\right\}. \tag{2}$$

The energy equation for flow in the saturated porous medium is given as

$$\rho C_p w^* \frac{\partial T}{\partial z^*} = \kappa_{\mathrm{e}}\Delta T + \Psi^*, \tag{3}$$

where T^*, ρ, C_p and κ_{e} respectively denote the fluid temperature, fluid density, specific heat capacity, and effective thermal conductivity of the fluid. The term Ψ^* is the contribution caused by viscous dissipation. The thermal boundary conditions are

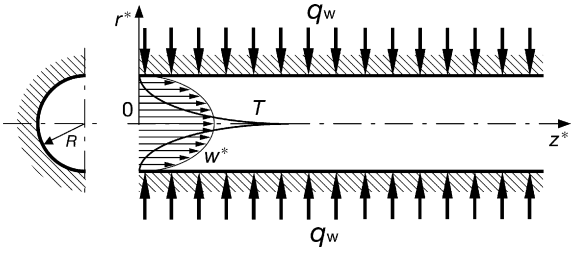

Fig. 1. Problem description.

$$\left.\begin{aligned}\left.\frac{\partial T}{\partial r^*}\right|_{r^*=0} &= 0\\ \kappa_e \left.\frac{\partial T}{\partial r^*}\right|_{r^*=R} &= q_w\end{aligned}\right\}; \tag{4}$$

we define nondimensional variables as

$$z = \frac{z^*}{R\cdot Pe}, \quad r = \frac{r^*}{R}, \quad M = \frac{\mu_e}{\mu}, \quad w = \frac{w^*}{w_m^*}, \tag{5}$$

where w_m^* is the mean flow velocity defined as

$$w_m^* = \frac{2}{R^2}\int_0^R w^* r^*\,dr^*. \tag{6}$$

Here the Peclet number, Pe, and the Reynolds number, Re, are

$$Pe = Re\,Pr = \frac{\rho C_p R w_m^*}{\kappa_e} \tag{7}$$

and

$$Re = \frac{\rho R w_m^*}{\mu}. \tag{8}$$

The nondimensional form of Eq. (1) is

$$M\frac{1}{r}\frac{\partial}{\partial r}\left(r\frac{\partial}{\partial r}\right)w - \frac{1}{Da}w + 1 = 0, \tag{9}$$

where Da is defined as

$$Da = \frac{K_p}{R^2}. \tag{10}$$

Because the fluid properties are assumed to be constant, i.e. independent of temperature, the solution of the flow field is decoupled from the thermal solution. Therefore, the solution of Eq. (9) subject to the boundary condition $w = 0$ at $r = 1$, and $dw/dr = 0$ at $r = 0$ is readily obtained as

$$w = \frac{\alpha I_0(\alpha)}{\alpha I_0(\alpha) - 2I_1(\alpha)}\left[1 - \frac{I_0(\alpha r)}{I_0(\alpha)}\right], \tag{11}$$

where $I_n(\alpha)$ and α respectively denote a modified Bessel function of nth order, and

$$\alpha = \frac{1}{\sqrt{MDa}}. \tag{12}$$

Furthermore, the nondimensional variable is defined as

$$\Theta = \kappa_e \frac{T - T_0}{q_w R}. \tag{13}$$

Several forms of the model have been proposed for description of the viscous dissipation term [10,11]. For the present study, we applied the viscous dissipation term recently proposed by Nield [12]:

$$\Psi^* = \frac{\mu}{K_p}w^{*2} - \mu_e w^* \Delta w^*. \tag{14}$$

Therefore, the nondimensional form of the energy equation is obtained by substituting Eqs. (13) and (14) into Eq. (3) as

$$w\frac{\partial \Theta}{\partial z} = \frac{1}{r}\frac{\partial}{\partial r}\left(r\frac{\partial}{\partial r}\right)\Theta + \frac{Br}{Da}\left[w^2 - \frac{1}{\alpha^2}\frac{w}{r}\frac{\partial}{\partial r}\left(r\frac{\partial}{\partial r}\right)w\right]. \tag{15}$$

Here, Br is the conventional Br [13]:

$$Br = \frac{\mu w_m^{*2}}{q_w R}. \tag{16}$$

The thermal boundary conditions in Eq. (4) are rewritten in nondimensional forms as

$$\left.\begin{aligned}\left.\frac{\partial \Theta}{\partial r}\right|_{r=0} &= 0\\ \left.\frac{\partial \Theta}{\partial r}\right|_{r=1} &= 1\end{aligned}\right\}. \tag{17}$$

Substitution of Eq. (11) into (15) yields the final form of the energy equation to be solved

$$\begin{aligned}&\frac{\alpha I_0(\alpha)}{\alpha I_0(\alpha) - 2I_1(\alpha)}\left[1 - \frac{I_0(\alpha r)}{I_0(\alpha)}\right]\frac{\partial \Theta}{\partial z}\\ &\quad = \frac{1}{r}\frac{\partial}{\partial r}\left(r\frac{\partial}{\partial r}\right)\Theta\\ &\qquad + \frac{Br}{Da}\left[\frac{\alpha I_0(\alpha)}{\alpha I_0(\alpha) - 2I_1(\alpha)}\right]^2\left[1 - \frac{I_0(\alpha r)}{I_0(\alpha)}\right].\end{aligned} \tag{18}$$

Eq. (18) is non-homogeneous; therefore, the solution Θ is expressible as the sum of a particular solution, θ, and the general (homogeneous) solution, θ_g

$$\Theta = \theta + \theta_g \tag{19}$$

Note that θ describes the axial variation of the local temperature, and θ_g describes the main decaying term given as an infinite series in terms of the eigenvalues and eigenfunction of the Sturm–Liouville type equation, similarly to the classical Graetz problem. First, to seek a particular solution, θ, we use the relation of the temperature gradient in the fully developed thermal condition:

$$\frac{\partial \Theta}{\partial z} = \frac{\partial \theta}{\partial z} = \frac{d\theta_m}{dz} \quad (z \to \infty; \theta_g = 0), \tag{20}$$

where θ_m is the bulk temperature. Therefore, Eq. (18) can be rewritten as

$$\begin{aligned}\frac{1}{r}\frac{\partial}{\partial r}\left(r\frac{\partial}{\partial r}\right)\theta &= \frac{\alpha I_0(\alpha)}{\alpha I_0(\alpha) - 2I_1(\alpha)}\left[1 - \frac{I_0(\alpha r)}{I_0(\alpha)}\right]\\ &\quad \times \left(\frac{d\theta_m}{dz} - \frac{Br}{Da}\frac{\alpha I_0(\alpha)}{\alpha I_0(\alpha) - 2I_1(\alpha)}\right).\end{aligned} \tag{21}$$

Integration of Eq. (21) with respect to r from 0 to 1, and the use of Eq. (17) yields the following result:

$$\frac{d\theta_m}{dz} = 2 + \frac{Br}{Da}\frac{\alpha I_0(\alpha)}{\alpha I_0(\alpha) - 2I_1(\alpha)} \tag{22}$$

Therefore, the bulk temperature variation along z-axis is obtained as

$$\theta_m = \left[2 + \frac{Br}{Da}\frac{\alpha I_0(\alpha)}{\alpha I_0(\alpha) - 2I_1(\alpha)}\right]z. \tag{23}$$

On the other hand, integration of Eq. (21) twice engenders the following result:

$$\theta = \frac{\alpha I_0(\alpha)}{\alpha I_0(\alpha) - 2I_1(\alpha)}\left(\frac{d\theta_m}{dz}\right)\left[\frac{1}{4}r^2 - \frac{I_0(\alpha r)}{\alpha^2 I_0(\alpha)}\right] + C, \tag{24}$$

where C is an integration constant. To determine the value of C, we used the alternative expression of the bulk temperature, θ_m, which is calculated from a heat balance over a cross-section of the circular tube. Consequently, θ_m becomes

$$\theta_m = 2\int_0^1 \theta w r\,dr = \frac{\{(\alpha^2+8)[\alpha I_0(\alpha)-4I_1(\alpha)]I_0(\alpha)+8\alpha[I_0^2(\alpha)-I_1^2(\alpha)]\}}{4\alpha[\alpha I_0(\alpha)-2I_1(\alpha)]^2} + C. \tag{25}$$

Therefore, the value of C is obtained as follows:

$$C = \left(2+\frac{Br}{Da}\frac{\alpha I_0(\alpha)}{\alpha I_0(\alpha)-2I_1(\alpha)}\right)z - \frac{\{(\alpha^2+8)[\alpha I_0(\alpha)-4I_1(\alpha)]I_0(\alpha)+8\alpha[I_0^2(\alpha)-I_1^2(\alpha)]\}}{4\alpha[\alpha I_0(\alpha)-2I_1(\alpha)]^2}. \tag{26}$$

Finally, the particular solution is obtained by substituting Eq. (26) into Eq. (24) as

$$\theta = \frac{2\alpha I_0(\alpha)}{\alpha I_0(\alpha)-2I_1(\alpha)}\left[\frac{1}{4}r^2-\frac{I_0(\alpha r)}{\alpha^2 I_0(\alpha)}\right] + \left(2+\frac{Br}{Da}\frac{\alpha I_0(\alpha)}{\alpha I_0(\alpha)-2I_1(\alpha)}\right)z - \frac{\{(\alpha^2+8)[\alpha I_0(\alpha)-4I_1(\alpha)]I_0(\alpha)+8\alpha[I_0^2(\alpha)-I_1^2(\alpha)]\}}{4\alpha[\alpha I_0(\alpha)-2I_1(\alpha)]^2}. \tag{27}$$

The general equation for θ_g is of the form ($Br = 0$ in Eq. (18))

$$\frac{\alpha I_0(\alpha)}{\alpha I_0(\alpha)-2I_1(\alpha)}\left[1-\frac{I_0(\alpha r)}{I_0(\alpha)}\right]\frac{\partial\theta_g}{\partial z} = \frac{1}{r}\frac{\partial}{\partial r}\left(r\frac{\partial}{\partial r}\right)\theta_g, \tag{28}$$

and the corresponding boundary conditions are

$$\left.\begin{aligned}\theta_g\big|_{z=0} &= \theta|_{z=0} = \frac{2\alpha I_0(\alpha)}{\alpha I_0(\alpha)-2I_1(\alpha)}\left[\frac{1}{4}r^2-\frac{I_0(\alpha r)}{\alpha^2 I_0(\alpha)}\right] - \frac{\{(\alpha^2+8)[\alpha I_0(\alpha)-4I_1(\alpha)]I_0(\alpha)+8\alpha[I_0^2(\alpha)-I_1^2(\alpha)]\}}{4\alpha[\alpha I_0(\alpha)-2I_1(\alpha)]^2}\\ \left.\frac{\partial\theta_g}{\partial r}\right|_{r=0} &= 0\\ \left.\frac{\partial\theta_g}{\partial r}\right|_{r=1} &= 0\end{aligned}\right\}. \tag{29}$$

Presume that the solution to Eq. (28) and (29) is of the form

$$\theta_g = \sum_{n=1}^{\infty} c_n R_n(r) e^{-\lambda_n^2 z}, \tag{30}$$

where c_n are the coefficients, $R_n(r)$ are the eigenfunctions, and λ_n are the eigenvalues. Substituting Eq. (30) into (28), we obtain the following nonlinear eigenvalue problem:

$$\frac{1}{r}\frac{\partial}{\partial r}\left(r\frac{\partial}{\partial r}\right)R_n(r)+\lambda_n^2\frac{\alpha I_0(\alpha)}{\alpha I_0(\alpha)-2I_1(\alpha)}\left[1-\frac{I_0(\alpha r)}{I_0(\alpha)}\right]R_n(r)=0, \tag{31}$$

with the boundary conditions

$$\left.\begin{aligned}\left.\frac{\partial R_n(r)}{\partial r}\right|_{r=0} &= 0\\ \left.\frac{\partial R_n(r)}{\partial r}\right|_{r=1} &= 0\end{aligned}\right\}. \tag{32}$$

Because Eqs. (31) and (32) constitute a Sturm–Liouville system, the series coefficient c_n is given as

$$c_n = \frac{\int_0^1 \Theta|_{z=0}[I_0(\alpha)-I_0(\alpha r)]R_n(r)r\,dr}{\int_0^1[I_0(\alpha)-I_0(\alpha r)]R_n^2(r)r\,dr}. \tag{33}$$

Eq. (31) were solved using the fourth-order Runge–Kutta method by varying the value of an eigenvalue to satisfy Eq. (32). This yields the accurate eigenvalue and the corresponding function is the required solution of Eq. (31). Once the eigenvalues and eigenfunctions have been obtained, c_n can readily be obtained by performing the integration of Eq. (33) numerically.

Therefore, the local Nu is given as

$$Nu = \frac{2}{\Theta|_{r=1}-\theta_m}. \tag{34}$$

3. Results and discussion

The analytical solutions were compared with numerical results [14] because there is no analytical solution of the heat transfer in a circular pipe saturated with a porous medium that accounts for the effects of viscous dissipation

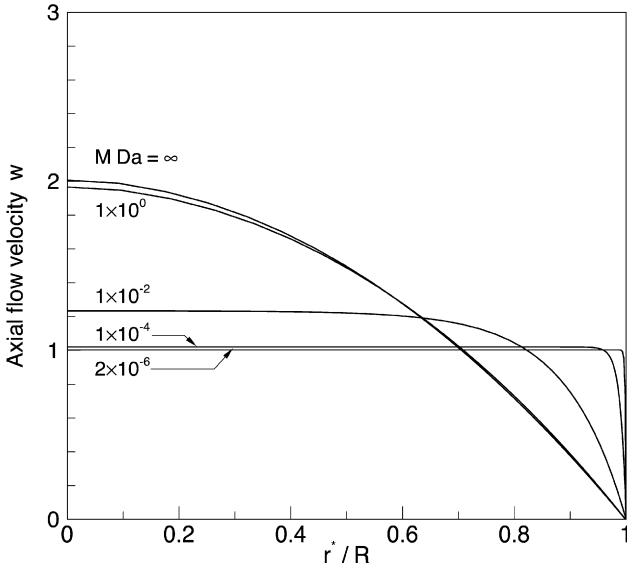

Fig. 2. Axial flow velocity profiles.

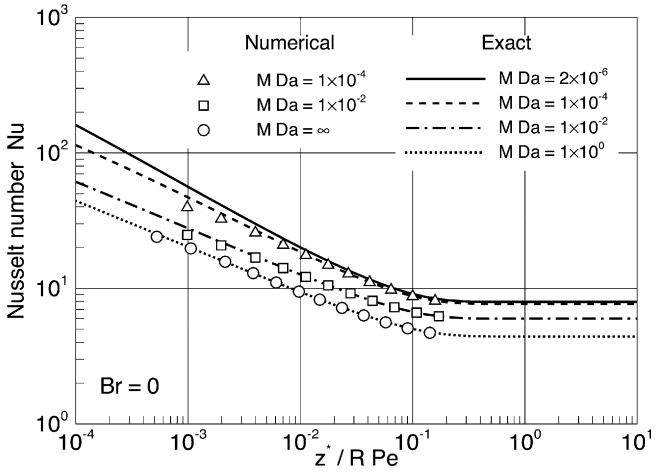

Fig. 3. Local Nu profiles along the tube at various values of MDa.

and constant wall heat flux. Fig. 2 shows profiles of the axial velocity (Eq. (11)) for five different values of MDa. In that figure, $MDa = \infty$ is the result for the plain Poiseuille flow.

Fig. 3 shows variations of the Nu (Eq. (34)) with nondimensional distance from the pipe entrance ($z = 0$) for various values of MDa for $Br = 0$ (without viscous dissipation) using 350 eigenvalues. Some representative values of the local Nu for various values of MDa are listed in Table 1 for convenience. For values of MDa smaller than 1×10^{-4}, the value of Nu in a log–log plot shows a departure from linear behavior as z approaches zero (not shown) because of insufficient number of eigenvalues used in evaluating the exact solution. The critical value of the axial position, $z(= z^*/RPe)$, the smallest value of z that gives the accurate Nu, was about $z_{crit} = 1 \times 10^{-5}$ for any MDa greater than $MDa = 2 \times 10^{-6}$ (in the case of $MDa = 2 \times 10^{-6}$; $z_{crit} \cong 5 \times 10^{-5}$). In the present study, it was difficult to obtain more eigenvalues than 350 because of rounding errors that resulted from the finite computer capacity. As a reference, it took about seven days to obtain 350 eigenvalues using a 128-CPU parallelized super computer Origin 2000. In the figure, numerical results [14] are shown for comparison. The results show good agreement with those of Nield et al. [15]. The value of $MDa = 2 \times 10^{-6}$ is the smallest value for which we were able to make the calculation and which approximates the case of Darcy (slag) flow. The fully developed value of 7.955 for $MDa = 2 \times 10^{-6}$ of the exact solution is close to the known value 8.000 [16] for the Darcy flow ($MDa = 0$).

Table 1
Nusselt number, Nu, for various values of MDa

Z^*/RPe	Nu				
MDa	2.0E−06	1.0E−04	1.0E−02	1.0E+00	1.0E+02
5.0E−05	217.227	145.894	77.277	55.897	54.791
1.0E−04	160.683	114.107	61.262	44.312	43.505
5.0E−04	77.384	61.885	35.302	25.673	25.274
1.0E−03	56.231	47.005	27.779	20.282	19.984
5.0E−03	27.104	24.510	15.971	11.800	11.646
1.0E−02	20.092	18.593	12.669	9.414	9.296
5.0E−02	10.962	10.484	7.825	5.870	5.802
1.0E−01	9.102	8.767	6.715	5.031	4.973
5.0E−01	7.958	7.699	5.988	4.421	4.367
1.0E+00	7.955	7.697	5.986	4.418	4.364
5.0E+00	7.955	7.697	5.986	4.418	4.364
1.0E+01	7.955	7.697	5.986	4.418	4.364

Fig. 4 shows the dependence of nondimensional wall temperature Θ_w on nondimensional distance from the pipe entrance, z^*/RPe for three different values of Br. The value of MDa remained constant at $MDa = 1 \times 10^{-2}$. Both analytical and numerical results show good agreement with each other. The wall temperature increases gradually along the downstream direction of the circular pipe before the flow field became thermally fully developed where the slope of the wall temperature become constant. However, the temperature field is remarkably altered when the value of the Br takes non-zero values. For values of $Br = 1 \times 10^{-2}$ and 1×10^{-1}, profiles of the wall temperature take higher values than that for $Br = 0$ at any locations because of the heat generation caused by viscous dissipation. For the value of $Br = 1 \times 10^{-2}$, the ratio of the amount of heat generation in the entire volume to that of the heat entry through the wall is small. For that reason, the effect of heat generation on the level of the wall temperature is minor. For the value of $Br = 1 \times 10^{-1}$, the wall temperature profile is largely deviated from that for $Br = 0$ because the heat transfer at the wall is dominated by heat generation caused by viscous dissipation. This dependence of the wall temperature profile on Br becomes considerable for smaller MDa because the viscous dissipation is considerable for flow in the porous medium with a quite low value of Da. Some representative values of the wall temperature, Θ_w, along the flow direction with a wide range of the MDa for values of $Br = 0$, 1×10^{-2}, and 1×10^{-1} are shown in Table 2 for convenience.

Temperature profiles in the cross-section of the circular pipe at different locations of z^*/RPe for three different

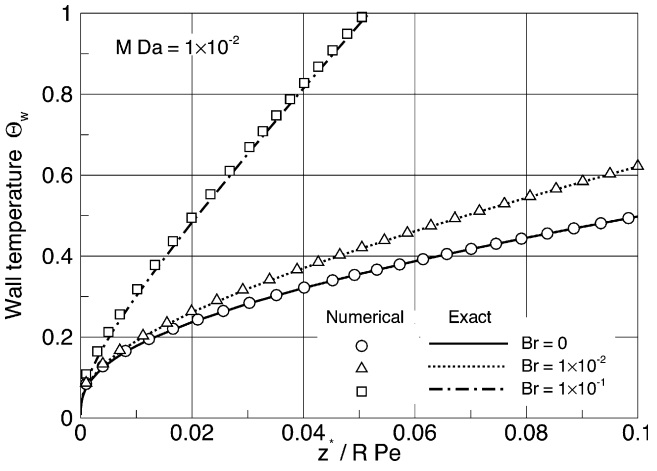

Fig. 4. Nondimensional wall temperature profiles along the tube at various values of Br.

Table 2
Wall temperature, Θ_W, for various values of MDa and Br

Z^*/RPe	MDa											
	1.0E−04			1.0E−02			1.0E+00			1.0E+02		
Br	0	0.01	0.1	0	0.01	0.1	0	0.01	0.1	0	0.01	0.1
1.0E−05	0.009	0.010	0.019	0.016	0.016	0.016	0.022	0.022	0.022	0.022	3.022	0.022
5.0E−05	0.014	0.019	0.065	0.026	0.026	0.027	0.036	0.036	0.036	0.037	3.037	0.037
1.0E−04	0.018	0.028	0.120	0.033	0.033	0.034	0.046	0.046	0.046	0.046	0.046	0.046
5.0E−04	0.033	0.084	0.543	0.058	0.058	0.064	0.079	0.079	0.080	0.080	1080	0.081
1.0E−03	0.045	0.147	1.065	0.074	0.075	0.086	0.101	0.101	0.102	0.102	1102	0.103
5.0E−03	0.092	0.602	5.193	0.135	0.141	0.197	0.180	0.180	0.184	0.182	1182	0.186
1.0E−02	0.128	1.148	10.331	0.178	0.190	0.301	0.233	0.234	0.242	0.235	3.236	0.243
5.0E−02	0.291	5.392	51.306	0.356	0.417	0.973	0.441	0.446	0.488	0.445	1449	0.485
1.0E−01	0.428	10.631	102.459	0.498	0.621	1.732	0.598	0.607	0.691	0.602	1610	0.682
5.0E−01	1.260	52.275	511.412	1.334	1.951	7.505	1.453	1.499	1.919	1.458	1.498	1.859
1.0E+00	2.260	104.290	1022.564	2.334	3.568	14.676	2.453	2.546	3.386	2.458	2.538	3.260
5.0E+00	10.260	520.412	5111.779	10.334	16.505	72.041	10.453	10.919	15.116	10.458	11859	14.465
1.0E+01	20.260	1040.564	10223.298	20.334	32.676	143.748	20.453	21.386	29.780	20.458	21.260	28.472

values of Br are shown in Fig. 5. The convergence of the infinite series is very slow at $r/R = 0$; therefore we plotted the results from $z^*/RPe = 0.002$. The temperature distributions in cross-sections at any location along the axial direction are strongly dependent on the value of Br as well as the wall temperature shown in Fig. 4. At any location, the wall temperature is higher than the fluid phase temperature to maintain a positive heat flux at the wall. For a larger value of $Br = 1 \times 10^{-1}$, the temperature field reaches the thermally fully developed condition in a short entrance length of z^*/RPe of ca. 0.02 because of the strong heat generation throughout the entire volume of the porous medium. Temperatures in the porous medium increase along the downstream direction, as shown previously in Fig. 4; the slope of the wall temperature profile for $Br = 1 \times 10^{-1}$ is almost constant at locations $z^*/RPe > 0.02$.

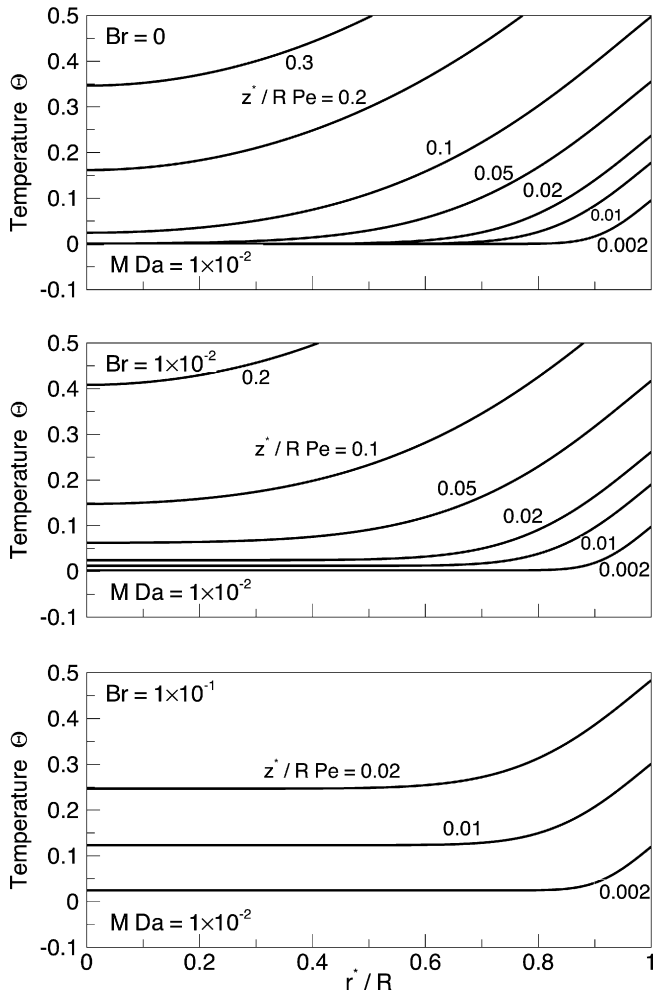

Fig. 5. Radial distribution of the temperature at Br: (top) $Br = 0$, (middle) $Br = 1 \times 10^{-2}$, (bottom) $Br = 1 \times 10^{-1}$.

Contours of the temperature difference, $\Theta - \theta_m$, for three different values of MDa are illustrated in Fig. 6. The value of Br remains constant at $Br = 1 \times 10^{-2}$. That figure shows the temperature distribution only within regions of $z^*/RPe < 0.2$ because the temperature field reaches a thermally fully developed condition at this location for any value of MDa in the present study. It is noteworthy that the temperature difference in the immediate vicinity of the wall increases as the value of MDa increases, implying that a larger value of the MDa renders the radial distribution of the temperature to be non-uniform for the simple reason that magnitudes of the first term of the viscous dissipation term used in the present study (Eq. (14)) are proportional to the value of the square of the axial velocity component. That value differs slightly from the conventional one that appears in momentum equations for the plain Poiseuille flow case. In other words, the spatial distribution of the heat generation caused by the viscous dissipation in the transverse direction to the flow becomes uniform as the value of MDa decreases because the radial distribution of the axial velocity changes its profile from a parabolic to a uniform distribution as the value of MDa decreases (see Fig. 2).

The local Nu based on the pipe radius is plotted against the longitudinal coordinate that was nondimensionalized in

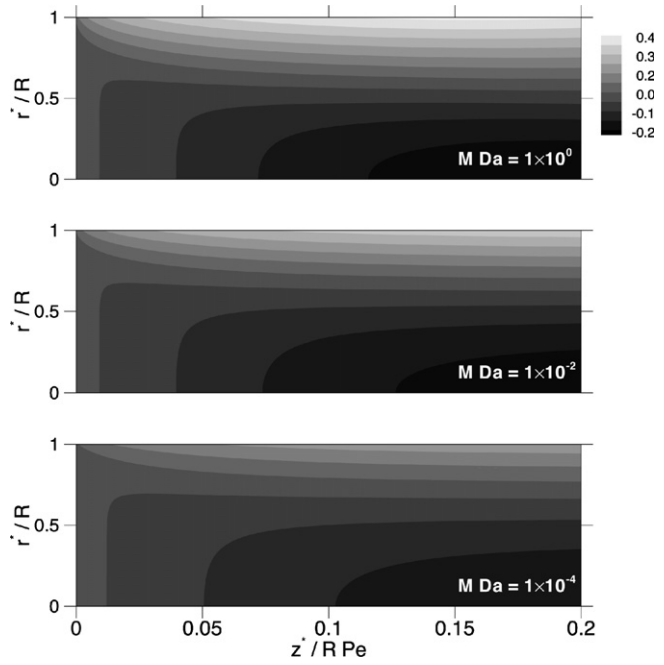

Fig. 6. Contours of temperature difference, $\Theta - \theta_m$, for three different values of MDa: (top) $MDa = 1$, (middle) $MDa = 1 \times 10^{-2}$, (bottom) $MDa = 1 \times 10^{-4}$.

terms of the pipe radius and Pe, z^*/RPe, in Fig. 7. The thin solid lines indicate exact solutions (Eq. (34)) with a wide range of MDa for various values of Br. Results of numerical computations for $MDa = 1 \times 10^{-2}$ are indicated (open symbols) for comparison. It is noteworthy that, for porous media, the local Nu is independent of the Br, even though the heat generation caused by the viscous dissipation of flow remarkably alters the temperature distribution, as shown previously. However, these findings should be interpreted with caution because the way of Nu dependence on Br is entirely different from different forms of the viscous dissipation term, except when the MDa takes a small value [5]. In the present study, we applied the most proper model

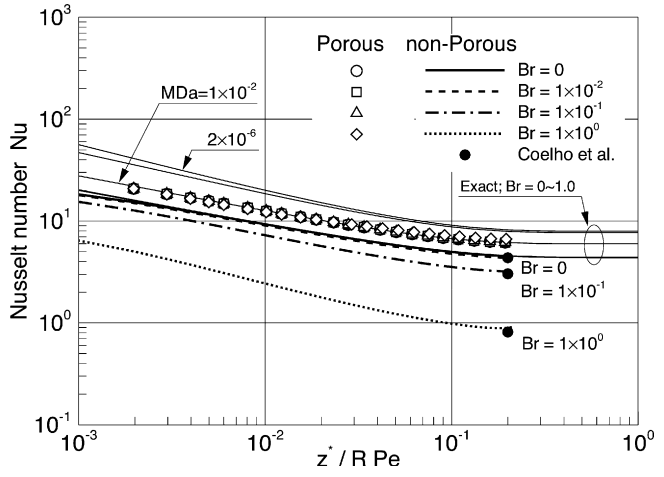

Fig. 7. Local Nu profiles along the axial direction at various values of the Br. Lines of the exact solution are, from the top, for $MDa = 2 \times 10^{-6}$, 1×10^{-4}, 1×10^{-2}, 1×10^{0}, 1×10^{2}.

for viscous dissipation in porous media [12]. However, the difference in the value of Nu among models is not significant for small MDa, which is adaptive for most porous materials. In addition, general features of heat transfer in porous media differ greatly from those of the plain Poiseuille flow as well. Thick lines (solid, dashed, dot-dashed, dotted) in Fig. 7 are plots of numerical results for the plain Poiseuille flow for different values of Br. As a reference, analytically obtained values of the local Nu for the thermally fully developed condition obtained by Coelho et al. [17] (closed circles) are shown together. For the plain Poiseuille flow, the local Nu decreased with increasing Br because the magnitude of the heat generation in the flow is proportional to the value of the square of the local axial velocity gradient. In the immediate vicinity of the wall, heat coming into the tube through the wall is transferred laterally only slightly toward the central core region because of the strong axial convective transport, which prevents heat from being transferred by the radial conduction transport. Therefore, the temperature rise in the core central region is not considerable when compared with the wall temperature, leading to the reduced value of the bulk temperature, which consequently reduces the value of the wall Nu (see Eq. (34)).

4. Summary

The governing equations for steadily developing forced convection in a circular tube filled with the saturated porous medium subjected to the boundary condition of the constant wall heat flux, with the viscous dissipation, were solved analytically. The solution was obtained using the method of separation of variables. The Sturm–Liouville system was solved to obtain the eigenvalues; ordinary differential equations for the eigenfunctions were calculated numerically using the fourth-order Runge–Kutta method. Results show that values of the local Nu evolution along the flow direction increase concomitant with decrease in the value of the MDa. However, values of the local Nu are independent of Br. The temperature profile is strongly dependent on the values of Br and MDa. Results also show that the effect of the viscous dissipation alters the transversal profile of the developing temperature field at any location in the tube because of the uniformly distributed heat sources of the dissipative term in the energy equation. This feature of the thermal behavior in porous media differs entirely from that in the plain Poiseuille flow case.

References

[1] D.A. Nield, A. Bejan, Convection in Porous Media, Third ed., Springer-Verlag, New York, 2006.
[2] A. Haji-Sheikh, K. Vafai, Analysis of flow and heat transfer in porous media imbedded inside various-shaped ducts, Int. J. Heat Mass Transfer 47 (2004) 1889–1905.
[3] D.A. Nield, A.V. Kuznetsov, M. Xiong, Thermally developing forced convection in a porous medium: parallel plate channel or circular duct with isothermal walls, J. Porous Media 7 (2004) 19–27.

[4] A.V. Kuznetsov, M. Xiong, D.A. Nield, Thermally developing forced convection in a porous medium: circular duct with walls at constant temperature with longitudinal conduction and viscous dissipation effects, Transport Porous Med. 53 (2003) 331–345.
[5] D.A. Nield, A.V. Kuznetsov, M. Xiong, Effects of viscous dissipation and flow work on forced convection in a channel filled by a saturated porous medium, Transport Porous Med. 56 (2004) 351–367.
[6] D.A. Nield, A.V. Kuznetsov, M. Xiong, Thermally developing forced convection in a porous medium: parallel plate channel with walls at uniform temperature, with axial conduction and viscous dissipation effects, Int. J. Heat Mass Transfer 46 (2003) 643–651.
[7] K. Hooman, A.A. Ranjbar-Kani, Viscous dissipation effects on thermally developing forced convection in a porous medium: circular duct with isothermal wall, Int. Commun. Heat Mass Transfer 31 (2004) 897–907.
[8] K. Hooman, A. Pourshaghaghy, A. Ejlali, Effects of viscous dissipation on Thermally developing forced convection in a porous saturated circular tube with an isoflux wall, Appl. Math. Mech. (English Edition) 27 (2006) 617–626.
[9] H.C. Brinkman, A calculation of the viscous force exerted by a flowing fluid on a dense swarm of particles, Appl. Scient. Res. A1 (1947) 27–34.
[10] A.K. Al-Hadhrami, L. Eliott, D.B. Ingham, A new model for viscous dissipation in porous media across a range of permeability values, Transport Porous Med. 53 (2003) 117–122.
[11] D.A. Nield, Comments on 'A new model for viscous dissipation in porous media across a range of permeability values', Transport Porous Med. 53 (2003) 117–122, Transport Porous Med. 55 (2004) 253–254.
[12] D.A. Nield, Resolution of a paradox involving viscous dissipation and nonlinear drag in a porous media, Transport Porous Med. 41 (2000) 349–357.
[13] D.A. Nield, A note on a Brinkman–Brinkman forced convection problem, Transport Porous Med. 64 (2006) 185–188.
[14] S. Tada, K. Ichimiya, Numerical simulation of forced convection in a porous circular tube with constant wall heat flux: extended Graetz problem with viscous dissipation, Chem. Eng. Technol., in review.
[15] D.A. Nield, A.V. Kuznetsov, M. Xiong, Thermally developing forced convection in a porous media: parallel-plate channel or circular tube with walls at constant heat flux, J. Porous Media 6 (2003) 203–212.
[16] K. Hooman, A.A. Ranjbar-Kani, A perturbation based analysis to investigate forced convection in a porous saturated tube, J. Comput. Appl. Math. 162 (2004) 411–419.
[17] P.M. Coelho, F.T. Pinho, P.J. Oliveira, Thermal entry flow for a viscoelastic fluid: the Graetz problem for the PTT model, Int. J. Heat Mass Transfer 46 (2003) 3865–3880.